Localized and Delocalized Charge Transport in Single-Wall Carbon-Nanotube Mats

O. Hilt and H. B. Brom

Kamerlingh Onnes Laboratory, Leiden University, P.O. Box 9504, 2300 RA Leiden, The Netherlands

M. Ahlskog

Low Temperature Laboratory, Helsinki University of Technology, FIN-02015 HUT, Finland

We measured the complex dielectric constant in mats of single-wall carbon-nanotubes between 2.7 K and 300 K up to 0.5 THz. The data are well understood in a Drude approach with a negligible temperature dependence of the plasma frequency ω_p and scattering time τ with an additional contribution of localized charges. The dielectric properties resemble those of the best "metallic" polypyrroles and polyanilines. The absence of metallic islands makes the mats a relevant piece in the puzzle of the interpretation of τ and ω_p in these polymers.

Depending on the wrapping of the graphene sheet, the intrinsic electronic properties of single-wall carbon-nanotubes (SWNTs) are either semiconducting (zigzag and most chiral nanotubes) or metallic (armchair and part of the chiral nanotubes) [1,2]. Single ropes of arm-chaired SWNTs as well as entangled networks (mats) show a decrease of the dc conductivity, σ_{dc}, with increasing temperature (T) for T above a critical temperature (T^*) [3–6]. For $T < T^*$, σ_{dc} decreases with cooling. T^* typically lies between 40 K and 250 K and depends on the morphology and the degree of disorder [4]. The transition from $d\sigma_{dc}/dT < 0$ to $d\sigma_{dc}/dT > 0$ at T^* is ascribed to structural defects and built-in impurities of the individual nanotubes [7,8], or to barriers between the nanotubes or ropes limiting the extension of the charge-carrier states [5]. Additional information about this issue can be obtained from frequency- dependent phase-sensitive permittivity experiments, giving the complex conductivity $\sigma(\omega) = \sigma'(\omega) + i\sigma''(\omega)$ or dielectric constant, $\epsilon(\omega) = \epsilon'(\omega) - i\epsilon''(\omega)$ [9]. Different frequency dependencies of σ' and ϵ' are expected for the two limiting cases of localized and delocalized charge transport and also the sign of ϵ' changes with the two models. Here we apply this method to mats of SWNTs. The data do not need Kramers-Kronig analysis, which is a great advantage for the analysis of the response of the delocalized charge carriers [10]. Like heavily doped polymers SWNTs are shown to be an example of a system with exceptional long scattering times τ and low plasma frequencies ω_p, but in contrast to the polymers metallic islands can be excluded as an explanation. For that reason SWNTs form an important new element in the not-yet understood physics behind τ and ω_p.

Weak inter-nanotube contacts or strong intra-nanotube defects might lead to charge localization. The motion of the localized charge carriers will be diffusion controlled and the frequency-dependent conductivity $\sigma(\omega) = (ne^2/k_B T)D(\omega)$ is given by linear response theory as [11]

$$D(\omega) = -\frac{1}{2d}\,\omega^2 \int_0^\infty \langle(r(t) - r(0))^2\rangle e^{-i\omega t} dt \qquad (1)$$

with d the dimensionality of the transport system, r the charge-carrier position and $\langle\rangle$ the configurational average. Eq. (1) reduces to Fick's law for a frequency independent D. With increasing frequency σ' will increase while the positive ϵ' decreases [12,13]. In the delocalized case charge transport is expected to follow the scheme of a Drude electron-gas with a conductivity:

$$\sigma(\omega) = \epsilon_0\,\omega_p{}^2\tau\,\frac{1}{1 + i\omega\tau} \qquad (2)$$

with $\omega_p^2 = nq^2/(\epsilon_0 m^*)$ [14]. For most metals $\omega_p \sim 10^{15}$ s^{-1}. If charge transport is governed by (anomalous) diffusion (Eq.(1)), $d\sigma'/d\omega \geq 0$ and $\epsilon' \geq 1$. In contrast, the Drude model of delocalized charge transport (Eq.(2)) predicts $\epsilon' < 0$ for $\omega \ll \omega_p$ and $d\sigma'/d\omega \leq 0$ and $d\epsilon'/d\omega \geq 0$ for $\omega \sim \tau^{-1}$.

SWNT mats [15] were prepared by vacuum-filtering a suspension of SWNT's in water with approx. 0.5 % Triton X-100, a non-ionic surfactant, through filter paper with a pore size of 1 μm. The SWNT's were produced using laser-ablation [16]. Purification of the mats was performed by washing the filter paper with the attached SWNT mat with deionized water to remove the Triton X-100 and with methanol to remove residual NaOH [17]. In this way, mats with a diameter of 34 mm and a thickness of typically 10 μm were obtained. Some of these SWNT mats were investigated with the filter paper attached to it. Other mats could be peeled off the filter paper. Up to now SWNT mats are always mixtures of chiral, zig-zag and armchaired nanotubes. The fraction of metallic nanotubes is estimated to be of the order of 0.1-0.5 [3,6,18]. For these strand-like materials such numbers are sufficiently high to be well above the percolation threshold for dc-conduction [13].

The dc conductivity (σ_{dc}) of the mats was measured with the four-probe technique. The T-dependent dc measurements were performed in an Oxford flow (down to 4

K) and a ^{3}He cryostat (down to 0.4 K). Complex $\sigma(\omega)$ or $\epsilon(\omega)$-data in the GHz regime were obtained by running-wave transmission-measurements with the electric-field vector parallel to the plane of the mat. The transmission and the phase shift introduced by the sample were directly measured with an ABmm millimeter-wave network analyzer. The complex dielectric constant at the given ω could be obtained by fitting the data to first principles formulae [19] without the need of a Kramers-Kronig analysis. The attenuation of the samples was approximately 45 dB. For the transmission experiments at 10 GHz and at 15 GHz, resp. X-band and P-band rectangular waveguides were used. The sample was mounted onto a choke flange of the waveguides. Between 40 GHz and 500 GHz a free-space electromagnetic wave, focused with polyethylene lenses was transmitting the SWNT mat. For the T-dependent measurements at 285 GHz the SWNT mat was mounted in an optical He-flow cryostat. The mm-wave reached the sample by passing two quartz and capton windows with a diameter of 40 mm. The sample space of the cryostat was filled with liquid He for measurements below 4.2 K. The resulting change of ϵ of the medium surrounding the sample was considered in the analysis.

In Fig. 1 the T dependences of $\sigma'_{285\mathrm{GHz}}$ and σ_{dc}, normalized to the 300 K value of 6.9×10^4 S/m for the cleaned and 2×10^4 S/m for the uncleaned SWNT mats are shown.
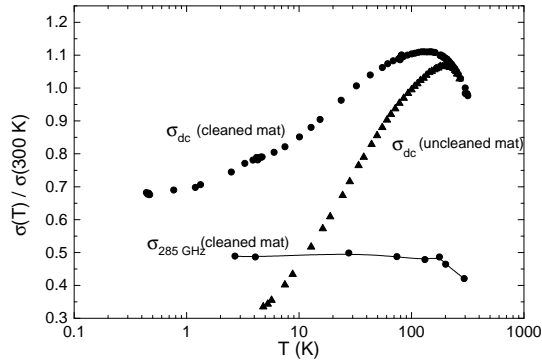
FIG. 1. Normalized T dependence of σ_{dc} (circles) and $\sigma'_{280\mathrm{GHz}}$ (open squares) for a cleaned SWNT mat. The triangles show $\sigma_{\mathrm{dc}}(T)$ for a desiccated mat.

Clearly visible is the change from a positive $d\sigma'/dT$ at low T to a negative $d\sigma'/dT$ at high T. The transition temperatures between the two regimes is close to $T^* = 120$ K in agreement with recently reported values for similar prepared SWNT mats [3] (for the uncleaned mat $T^* \sim 200$ K). The measured frequency dependences of ϵ' and σ' show the following main features, see Fig 2: the conductivity almost keeps its dc value up to about 10 GHz and decreases at higher frequencies. Saturation is observed close to 1 THz. The dielectric constant increases from $\epsilon' \sim -10^4$ in the 10 GHz-regime

to $\epsilon' \sim -100$ close to 1 THz, apparently approaching the regime of $\epsilon' > 0$ at still higher frequencies.
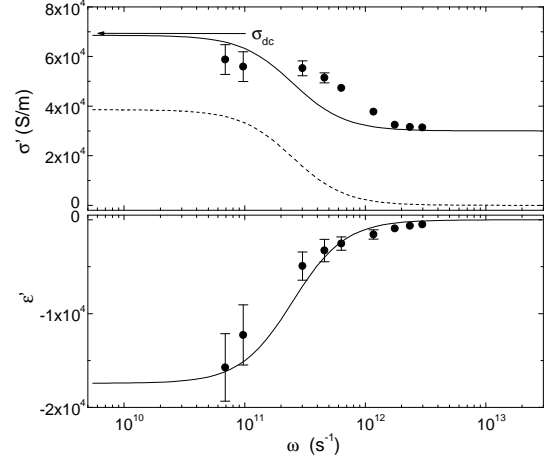

FIG. 2. Dependence on ω of ϵ' and σ' for cleaned SWNT mats at 300 K (full circles). The arrow marks σ_{dc}. Lines are fits with a Drude model ($\tau = 4.0$ ps and $\omega_p = 3.3 \times 10^{13}$ s^{-1}) without (dashed line) and with (full line) background conductivity $\sigma_b = 3 \times 10^4$ S/m.

The dielectric constant at 285 GHz remains negative down to 2.7 K, see the temperature-dependent data in Fig. 3. For $T > T^*$, $\sigma'_{285\mathrm{GHz}}(T)$ is proportional to $\sigma_{\mathrm{dc}}(T)$. For $T < T^*$, $\sigma'_{285\mathrm{GHz}}(T)$ remains constant, while $\sigma_{\mathrm{dc}}(T)$ decreases with decreasing T, see Fig. 1.
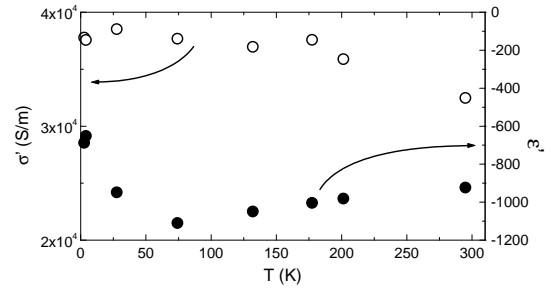

FIG. 3. T dependence of σ' (open circles) and ϵ' (full circles) for cleaned SWNT mats between 2.7 K and 300 K at 285 GHz.

To study the influence of inter-rope barriers, desiccated SWNT mats were prepared by evaporating the water after casting the suspension onto a quartz substrate. After desiccation, the remaining surfactant covers the SWNT-ropes. Fig. 4 shows the dielectric constant to be positive for such an unpurified SWNT mat. After rinsing the mat with deionized water and methanol, the charge-transport properties turned from a localized-carrier dominated regime with $\epsilon' > 0$, $d\epsilon'/d\omega < 0$ and $d\sigma'/d\omega > 0$ for the unpurified sample to a delocalized-carrier dominated (metallic) regime with an increased σ_{dc}, $\epsilon' < 0$, $d\epsilon'/d\omega < 0$ and $d\sigma'/d\omega < 0$, see Fig. 4.
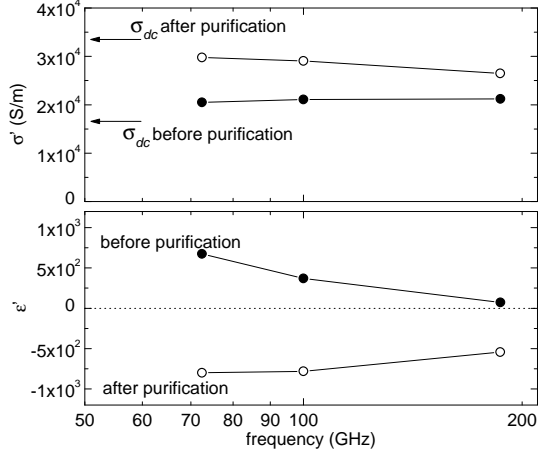
2

FIG. 4. Frequency dependence of σ' and ϵ' for a desiccated SWNT mat before (full circles) and after (open circles) purification at 300 K. The charge transport is dominated by localized carriers in the unpurified mat and shows metallic properties after purification.

The peculiar T dependence of σ_{dc} has been explained as a transition from metallic charge-transport at high temperatures to a non-metallic regime at low temperatures caused by charge-transport barriers of the order of some 10 meV [20]. Such a model is expected to give a thermally activated behavior of the conductivity at very low temperatures. In our data (see Fig. 1) $\sigma_{dc}(T)$ flattens below 10 K showing the model to be too crude. The metallic nature at room temperature is supported by the negative dielectric constant obtained from the high-frequency dielectric measurements, and $d\sigma'/d\omega \leq 0$ and $d\epsilon'/d\omega \geq 0$ for $\omega \sim \tau^{-1}$, see Fig. 2. A qualitative discrepancy between the observed frequency dependencies and the Drude behavior lies in the saturation of σ' for $\omega > \tau^{-1}$. The high-frequency conductivity remains at approx. 40 % of σ_{dc}. This points to a background-conductivity, σ_b, due to localized charge carriers present in the system. A possible increase with frequency of this background [21] (here neglected) will enhance the Drude response at the lowest frequencies at most by a factor of 2. The positive contribution to ϵ' (also neglected) is usually well below 10^3 in the GHz-regime and decreases with ω.

A fit of the Drude model including background conductivity is shown in Fig. 2. At low frequencies the value of σ' is not accurate and the experimental error of ϵ' in the 10 GHz-range is considerable. Although discrepancies in the shape of the frequency dependencies remain, the principal characteristics as described above can be reproduced. The observed more stretched frequency dependence is expected for a distribution of τ and ω_p. Given the experimental inaccuracies, the order of magnitude of the fit parameters is correct. The scattering time is estimated as $\tau = 2 - 5 \times 10^{-12}$ s, the plasma frequency as $\omega_p = 2.5 - 5.5 \times 10^{13}$ s^{-1} and the background conductivity as $\sigma_b = 2 - 3 \times 10^4$ S/m.

Using the Fermi velocity of graphite, $v_F = 8 \times 10^5$ m/s, the scattering time τ gives a mean free path of $\Lambda \sim 3$ μm. A similar value has been estimated from ESR measurements at 100 K on SWNT mats [6]. From DC measurements on an isolated SWNT at a few mK $\Lambda = 3$ μm is suggested as a lower limit [22]. Although theoretical arguments [23] predict a very low scattering probability with acoustic phonons inside a tube, which might allow similar values also at higher temperatures, the Λ found here refers to 3D transport, for which such a value seems (far) too high. We will return to this problem below.

The obtained plasma frequency is about one percent of ω_p for normal metals. Assuming $m^* = m_e$, the value of ω_p implies a charge-carrier density $n = 3 - 9 \times 10^{23}$ m^{-3}. Correcting for the lower density of the mats (~ 0.65 g/cm^3) compared to that of a SWNT (~ 2 g/cm^3) and assuming a fraction of 50% metallic tubes [6] would give $n \sim 4 \times 10^{24}$ m^{-3}, comparable to graphite. However, for SWNT n is predicted to be about $10^2\times$ higher [24]. Fischer et al. [3] found after mass-density corrections a more than $10\times$ higher σ_{dc} for single ropes than for mats. It is plausible that in a mat only a fraction of the charge carriers present participate in the delocalized (metallic) charge transport, while due to localization the remaining charge carriers have a smaller contribution to σ_{dc} [25]. In the model proposed here localized charge carriers are incorporated and contribute to σ_b.

At $T = 300$ K $\sigma'_{285\text{GHz}}$ is mainly due to σ_b, i.e. localized charge carriers (see fit in Fig.2). At such a high frequency $\sigma'(\omega)$ might well be determined by photon- instead of phonon-assisted hopping [26,21], which explains the constant value of $\sigma'_{285\text{GHz}}(T)$ for $T \leq 10^2$ K . However, ϵ' is still dominated by the delocalized charges over the whole temperature range ($\epsilon' < 0$ at 285 GHz, Fig. 3). The decrease by 40 % of $|\epsilon'|$ between 70 K and 2.7 K can be accounted for by the decrease of carriers from the semiconducting tubes and a growing contribution of localized states. It shows that the metallic part of $\epsilon'(\omega)$ for $\omega > 1/\tau$ has no strong T dependence, which implies an almost T independence of ω_p. Also σ_{dc} at 0.4 K is only a factor 0.7 lower than at 300 K, which indicates that not only ω_p but also τ have not changed appreciably with T. An opening of a gap due to twistons in the order of 20 meV as suggested by Kane and Mele [20] seems therefore unlikely. Based on the measured metallic low-temperature behavior down to 4.2 K of the thermoelectric power in SWNT ropes, Hone et al. [27] also excluded the opening of a gap at low T [28].

The room temperature data presented in Fig. 4 confirm the importance of inter-rope contacts at low temperatures. The purification procedure removed the surfactant and other impurities from the surface of the SWNT ropes allowing better contacts between ropes. Intra-tube or intra-rope transport are likely not changed by the purification, meaning that charge-localization effects due to defects in the graphene-sheet pattern of the tubes or bending of them should be unaffected. The effect of the purification on $\sigma_{dc}(T)$, see Fig. 1, supports the picture.

The transition temperature T^* for the uncleaned sample is higher than for the cleaned one. Also, $d\sigma_{dc}/dT$ below T^* is larger for the latter. Both indicate that inter-rope barriers limit σ_{dc} at low temperatures. These findings are consistent with the higher σ_{dc}, lower T^* and weaker $d\sigma_{dc}/dT$ below T^* [3] of single rope data, where inter-rope barriers are eliminated.

Highly conducting polymers like doped polyaniline (PAN) and polypyrrole (PPy) [29,30] and SWNT-mats show analogous dielectric behavior. In the metallic polymers σ_{dc} typically has a maximum value of order 10^4 S/m (around 200 K) and decreases to lower temperatures. The values of $\epsilon'(\omega)$ are strongly frequency and T dependent. Let us take one of the best conducting materials, PAN doped with d,1-camphorsulfonic acid (PAN-CSA), as an example [30]. Around 1 meV ($\omega \sim 1.5$ THz) at 200 K $\epsilon'(\omega)$ is a few times -10^3, and becomes less negative at lower T. For the same samples at room temperature $\epsilon'(\omega)$ starts negative, becomes positive around 30 meV, returns negative around 0.1 eV and finally comes close to zero in the optical regime. In the SWNT-mats the maximum value of σ_{dc} is almost 10^5 S/m, and $\epsilon(285$ GHz$)$ reaches a value of -10^3 and decreases in absolute value with decreasing temperature (by a factor of two at 4.2 K). At room temperature below 0.5 meV $\epsilon'(\omega)$ is negative, likely becomes positive at higher energies and returns negative again around 10 meV [18,31,10]. The comparison shows that best conducting polymers are essentially behaving like well-rinsed mats of single wall nanotubes (the same similarity exists between not-rinsed mats and the slightly less conducting polymers). Like in the mats, in these polymers values for Λ will be of the order of 100 nm for $v_F = 5 \times 10^5$ m/s [30]. In the metallic polymers homogeneous and inhomogeneous disorder models [30,10] are frequently used to explain these extreme values. For the nanotubes crystalline regions are excluded (TEM pictures show the nanotube mats to be completely entangled and disordered), which at least for the SWNT-mats requires an alternative for the inhomogeneous disorder model.

In summary, we have shown that the delocalized properties of nanotube mats can be completely determined by sub-THz measurements and are well described in a Drude picture with a negligible temperature dependence of the plasma frequency and scattering time. The values of ω_p and τ resemble those found in well conducting doped polymers. When modeled with the usually chosen Fermi velocities, unusually large values of the mean free path result for both systems. This finding and the absence of crystalline regions in the mats underline the need for a better description of these disordered strand-like systems.

[1] N. Hamada, S. Sawada and A. Oshiyama, Phys. Rev. Lett. **68**, 1579 (1992).
[2] J.W.G. Wildöer et al., Nature **391**, 59 (1998).
[3] J. E. Fischer et al., Phys. Rev. B **55**, R4921 (1997).
[4] C. L. Kane et al., Europhys. Lett. **41**, 683 (1998).
[5] A. B. Kaiser et al., Phys. Rev. B **57**, 1418 (1998).
[6] P. Petit et al., Phys. Rev. B **56**, 9275 (1997).
[7] M. S. Fuhrer et al., Sol. Stat. Comm. **109**, 109 (1999).
[8] R.S. Lee et al., Nature (London) **388**, 255 (1997).
[9] $\epsilon_0\epsilon''(\omega) = \sigma'(\omega)/\omega$ and $\epsilon_0(\epsilon'(\omega) - 1) = \sigma''(\omega)/\omega$.
[10] B. Chapman et al. Phys. Rev. B **60**, 13479 (1999).
[11] H. Scher and M. Lax, Phys. Rev. B **7**, 4491 (1973).
[12] W. Schirmacher, Ber. Bunsenges. Phys. Chem. **95**, 368 (1991).
[13] L.J. Adriaanse et al., Phys. Rev. Lett. **78**, 1755 (1997).
[14] N.W. Ashcroft and N.D. Mermin, "Solid State Physics", Saunders College Publishers, Fort Worth (1976).
[15] The nanotube-solutions were provided by Tubes@Rice.
[16] A. Thess et al., Science **273**, 483 (1996).
[17] A. G. Rinzler et al., Appl. Phys. A **67**, 29 (1998).
[18] A. Ugawa, A.G. Rinzler, and D.B. Tanner, Phys. Rev. B **60**, R11305 (1999).
[19] J. A. Reedijk et al., to be published in Rev. Sci. Instr.
[20] C. Kane and E.J. Mele, Phys. Rev. Lett. **78**, 1932 (1997).
[21] J.A. Reedijk et al., Phys. Rev. B **57** R15116 (1998).
[22] S.J. Tans et al., Nature (London) **386**, 474 (1997).
[23] A.A. Farajian et al., Phys. Rev. Lett. **82**, 5084 (1999).
[24] J.W.Mintmire et al., Phys. Rev. Lett. **68**, 631 (1992).
[25] A. Bezryadin et al., Phys. Rev. Lett. **80**, 4036 (1998).
[26] H. Böttger and V.V. Bryskin, "Hopping Conduction in Solids", Akademie-Verlag, Berlin (1985).
[27] J. Hone et al., Phys. Rev. Lett. **80**, 1042 (1998).
[28] In these 3-dimensional mats of SWNTs we do not expect to see the typical one-dimensional characteristics of isolated armchair-SWNT behavior, see R. Egger and A.O. Gogolin, Phys. Rev. Lett. **79**, 5082 (1997), and C. Kane, L. Balents and M.P.A. Fisher, Phys. Rev. Lett. **79**, 5086 (1997).
[29] K. Lee, R. Menon, C.O. Yoon and A.J. Heeger, Phys. Rev. B **52**, 4779 (1995).
[30] R.S. Kohlman et al., Phys. Rev. Lett. **77**, 2766 (1996), id.. **78**, 3915 (1997).
[31] Recently Ugawa et al. [18] found negative values of ϵ above 100 cm^{-1} or 0.1 eV, which is higher than the plasma energy of 0.02 eV found here. These results can be reconciled by adopting the picture that already in the far infrared localized states dominate, or point to essential differences between the mats.